

Vehicle Redistribution in Ride-Sourcing Markets using Convex Minimum Cost Flows

Renos Karamanis, Eleftherios Anastasiadis, Marc Stettler and Panagiotis Angeloudis

arXiv:2006.07919v1 [cs.DS] 14 Jun 2020

Abstract—Ride-sourcing platforms often face imbalances in the demand and supply of rides across areas in their operating road-networks. As such, dynamic pricing methods have been used to mediate these demand asymmetries through surge price multipliers, thus incentivising higher driver participation in the market. However, the anticipated commercialisation of autonomous vehicles could transform the current ride-sourcing platforms to fleet operators. The absence of human drivers fosters the need for empty vehicle management to address any vehicle supply deficiencies. Proactive redistribution using integer programming and demand predictive models have been proposed in research to address this problem. A shortcoming of existing models, however, is that they ignore the market structure and underlying customer choice behaviour. As such, current models do not capture the real value of redistribution. To resolve this, we formulate the vehicle redistribution problem as a non-linear minimum cost flow problem which accounts for the relationship of supply and demand of rides, by assuming a customer discrete choice model and a market structure. We demonstrate that this model can have a convex domain, and we introduce an edge splitting algorithm to solve a transformed convex minimum cost flow problem for vehicle redistribution. By testing our model using simulation, we show that our redistribution algorithm can decrease wait times up to 50% and increase vehicle utilization up to 8%. Our findings outline that the value of redistribution is contingent on localised market structure and customer behaviour.

Index Terms—Ride-Sourcing, Vehicle Redistribution, Network Optimisation

I. INTRODUCTION

RIDE-sourcing companies, also referred to as Transportation Network Companies (TNCs) gradually dominated the pre-existing taxi market over the past decade, with evidence of their immense success stipulated in market analytics of urban transport data such as in New York City. [1]. TNCs often encounter imbalances in the supply and demand for rides. Such imbalances can increase customer wait times in areas where there is an under-supply of drivers, thereby decreasing the quality of service and the popularity of the platform. To mediate this effect, TNCs apply dynamic pricing strategies, usually in the form of variable surge pricing multipliers [2]. These dynamic pricing strategies by design motivate drivers to redistribute to under-served areas and suppress demand from customers whom their willingness to pay is exceeded [3].

The anticipated launch of autonomous vehicles in TNC services to cut operational costs could transform TNCs from

R. Karamanis, E. Anastasiadis, M. Stettler and P. Angeloudis are with the Department of Civil and Environmental Engineering, Imperial College London, UK, e-mail: renos.karamanis10@imperial.ac.uk.

matching platforms to fleet operators having complete control of the supply [4]. In such a scenario, currently implemented dynamic pricing strategies would still suppress demand [5], but TNCs, as fleet owners, would need to decide vehicle redistribution operations. Generally, in the absence of drivers entering the market proactively by knowing historical surge pricing patterns [2], autonomous vehicle ride-sourcing operators would need to manage their fleet effectively, to alleviate any asymmetries of demand across road-networks.

Fleet management, and especially empty vehicle redistribution, although not prevalent in ride-sourcing markets, has been an established practice in shared mobility (bike and car-sharing) [6], [7]. In existing shared mobility schemes, vehicle redistribution is carried out by dedicated staff. In the case of autonomous ride-sourcing, platforms would be able to instruct vehicles to self-relocate, thereby avoiding dedicated staff costs. TNCs could also proactively decide vehicle redistribution operations by exploiting the diverse area of predictive algorithms and existing data.

Nonetheless, this seamless autonomous vehicle relocation would endure mileage costs. Besides, increased fleet mileage can induce externalities such as congestion subject to fleet adoption rates [8]. Furthermore, as ride-sourcing markets are competitive, and travellers encounter alternative options, redistributed vehicles in an area are not guaranteed an assignment. Consequently, vehicle redistribution models which take account of relocation costs, local market structure and travel behaviour are paramount in assessing the value of vehicle redistribution to autonomous ride-sourcing platforms.

Research on taxi economics, such as the work in [9], has been seminal in influencing the implementation of spatio-temporal characteristics when modelling taxi markets. The authors in [9] did assume the flow of taxis in neighbouring areas; however, the work focused on evaluating system performance metrics for regulatory frameworks. Later studies also considered optimizing redistribution in shared mobility schemes such as bike-sharing or car-sharing¹ fleets [6], [7], [11], [12].

The structural differences² between ride-sourcing and traditional vehicle sharing schemes prohibited the direct application of such models in the ride-sourcing market. Vehicle redistribution for ride-sourcing/taxi markets became popular alongside the concept of autonomy. As a consequence, researchers inves-

¹For a comprehensive review of vehicle redistribution algorithms for car-sharing we refer readers to [10]

²In traditional shared mobility schemes vehicles are usually parked at designated stations, and dedicated staff performs the relocation. Also, vehicles are usually booked in advance.

tigated vehicle redistribution in simulation studies implementing simplified redistribution heuristics for shared autonomous vehicles [8], [13]. These studies were critical in identifying the extra mileage and congestion, respectively, when redistributing empty shared autonomous vehicles.

Recent research focused on identifying redistribution strategies for ride-sourcing operations either using demand predictions and integer programming or by exploiting queuing theoretical models to identify steady-state relocation strategies. In [14] a closed Jackson network was used to simulate an autonomous mobility-on-demand (MoD) service with passenger loss. The authors then solved the vehicle rebalancing problem using a linear program. Using a queuing-theoretical implementation, they showed that congestion effects due to rebalancing could be avoided. The authors in [15] replaced the Jackson network with a Baskett–Chandy–Muntz–Palacios (BCMP) queuing network model and considered vehicle charging operations.

The authors in [16] and [17] used reinforcement learning to identify rebalancing actions in an MoD scheme and ride-sourcing platform respectively and showed that their methods achieve effective rebalancing strategies. A fluid-based optimization problem on a queuing network was used in [18] to identify an optimal routing policy with an upper bound for empty car routing in ride-sharing systems. The study in [19] considered a Markov decision process for the problem of vacant taxi routing with e-hailing. The authors solved their model using an iterative algorithm to maximize the expected long-term profit over a working period.

The authors in [20] and [21] used predictive algorithms to estimate incoming requests and an integer programming model to assign idle vehicles to clustered regions. Their models were tested in a simulation of the New York City taxi data and achieved a significant reduction of waiting times. Model predictive control for vehicle redistribution was also utilized in [22] to utilize short term estimations of customer demand. The model in [22] achieved a significant reduction in waiting times when tested in simulation using Didi data.

The majority of relevant studies on vehicle redistribution (Table I) do not consider acumen in customer behaviour. The two main approaches are, assuming unassigned customers abort the platform immediately (passenger loss) or setting a maximum customer wait time (maximum wait), after which all customers abort the service. However, in realistic ride-sourcing implementations, potential customers would encounter alternative travel options based on the market structure, thereby deciding their mode choice based on several factors. Consequently, oversimplified models of customer behaviour and poor or nonexistent representation of market structure do not reflect the real value and cost of redistribution, since vehicle relocations do not necessarily result in guaranteed customers.

To address this literature gap, we present a mathematical programming formulation that accounts for market structure and customer choice behaviour. We model the derived vehicle redistribution problem as a non-linear minimum cost flow problem and prove that the model can have an optimal solution in a convex domain. We transform the non-linear model to the convex minimum cost flow problem and solve it using an

TABLE I
RELEVANT STUDIES ON VEHICLE REDISTRIBUTION

| Study | Method | Redistribution Cost | Customer Behavior |
|------------|--|------------------------------|----------------------------------|
| [14], [15] | Queuing theory Reinforcement Learning | Congestion Distance-based | Passenger loss Passenger loss |
| [16] | Reinforcement Learning | Fuel-based | Not-specified |
| [17] | Learning | Time-based | Passenger loss |
| [18] | Queuing theory | Time-based | Passenger loss |
| [19] | Markov decision process | Time-based | Not-specified |
| [20] | Demand prediction, integer programming | Passenger delay | Maximum wait |
| [21] | Demand prediction, integer programming | Time-based | Maximum wait |
| [22] | Demand prediction, integer programming | Time and Distance-based | No passenger loss |

edge-splitting pseudo-polynomial algorithm.

Our contribution is summarised as follows:

- 1) We incorporate customer choice and market structure in the vehicle redistribution problem.
- 2) We model the vehicle redistribution problem as a Non-Linear Minimum Cost Flow problem.
- 3) We derive a convex space for the problem and transform it into a Convex Minimum Cost Flow Problem, which is solved using a pseudo-polynomial algorithm edge splitting algorithm.

The remainder of this paper is structured as follows: In section II, we outline the structure of our proposed vehicle redistribution model as a non-linear minimum cost flow model. We then prove the existence of a convex region and present our edge-splitting solution algorithm. In section III we test our redistribution methodology in an agent-based model of using taxi data from New York City. Conclusions and recommendations for further work are provided in section IV.

II. METHODOLOGY

A. Vehicle Redistribution Problem

We consider an autonomous vehicle ride-sourcing fleet operator, opposed with the problem of identifying an allocation of vehicles to various operations to minimise the fleet's operational cost. The fleet operator identifies allocations of the vehicles at regular decision periods and operates in an urban road network split into different clusters.

At the beginning of each period, the operator identifies the vehicle counts in each cluster³. We choose the length τ of the decision epochs so as for the vehicles' state and location to only depend on the decisions made on the previous state. At each decision epoch, the fleet operator needs to allocate the vehicles in each cluster into three possible operational states; available for trip allocation, empty redistribution, or idle.

Vehicles assigned for trip allocation are immediately available for trip requests originating from their existing cluster, and their number depends on demand estimates for the commencing period. Empty redistribution refers to vehicles

³Vehicles soon to be located in a cluster are also included.

allocated for empty travel to other clusters to satisfy demand estimates for the commencing and subsequent periods. Finally, idle vehicles remain inactive in their initial cluster for the commencing period and act as reserve capacity for the fleet if required.

Consequently, vehicles are allocated from their initial state and clusters into the various operations at the beginning of the decision period and end up in updated states and clusters for the subsequent period. For convenience, we refer to the updated vehicle states as resulting states and the operational states as decision states.

We define the set of road network clusters J and assume the fleet operator has estimates of the total demand Z_{ij}^t from cluster i to cluster j for each $i, j \in J$ and for every time epoch $t \in T$. We assume the mean utility of travel in time epoch t for autonomous ride-sourcing trips from cluster i to cluster j for each $i, j \in J$ is realised using the following generalised cost function:

$$u_{ij}^t(x) = -\bar{v}(w_{ij}^t(x) + r_{ij}^t) - pr_{ij}^t \quad \forall i, j \in J, \forall t \in T \quad (1)$$

Where \bar{v} in (1) is the mean value of time of the ride-sourcing travellers, $w_{ij}^t(x)$ is the average wait time from request to pick up for a trip originating in cluster i and terminating in cluster j at period t for a supply of vehicles x , r_{ij}^t is the travel time from cluster i to cluster j during period t and p is the price per time for the service.

As mentioned in section I, various studies attempted to estimate service quality for ride-sourcing platforms using queuing theoretical models. In a queuing-theoretical concept, the service time is a monotonically decreasing convex function⁴ of the number of servers (supply x) using inputs such as the rate of requests per time (demand Z_{ij}^t) and the average service time (length of epoch t). For modelling convenience, assuming the average service time is similar to the length of epoch t , we define the wait time $w_{ij}^t(x)$ using an inverse function of vehicle supply, which maintains the monotonically decreasing convex properties of wait time used in the literature:

$$w_{ij}^t(x) = \frac{\alpha Z_{ij}^t}{x + 1} \quad \forall i, j \in J, t \in T, x \in \mathbb{R}^+ \quad (2)$$

Where α in equation (2), is a parameter to be determined via calibration with $\alpha \in \mathbb{R}_{>0}$. We regard α as proportional to the average time a client waits for pickup in a cluster once assigned to an empty vehicle in the cluster. As such, α is related to the cluster size and average velocity. By utilising a discrete choice model and assuming constant values for r_{ij}^t and p_{ij}^t in each period, we can calculate the proportion of travellers $q_{ij}^t(x)$ choosing the ride-sourcing fleet as an option to travel from cluster i to cluster j for a period t .

$$q_{ij}^t(x) = \frac{e^{u_{ij}^t(x)}}{e^{u_{ij}^t(x)} + \sum_{w \in W} e^{U_{ij}^{tw}}} \quad \forall i, j \in J, \forall t \in T \quad (3)$$

Where W in (3) refers to the set of alternative ride-sourcing options and U_{ij}^{tw} is the mean utility of option $w \in W$ for

⁴The convexity is valid as long as the number of servers exceeds a minimum threshold.

travelling from cluster i to cluster j in period t . As such, the number of travellers $N_{ij}^t(x)$ choosing the ride-sourcing service at period t to travel from cluster i to cluster j for a supply of vehicles x is found using the following equation:

$$N_{ij}^t(x) = q_{ij}^t(x)Z_{ij}^t \quad \forall i, j \in J, \forall t \in T \quad (4)$$

Equation (3) is a sigmoid function, as we can represent it in the form of the logistic function. Equation (4) is a scaled version of the sigmoid function in (3). Consequently, due to its non-linearity and monotonically increasing nature, the function for the number of travellers choosing the service $N_{ij}^t(x)$ does not necessarily match the supply of vehicles x .

B. Non-Linear Minimum Cost Flow Formulation

We propose a minimum cost flow formulation to solve the vehicle redistribution problem described in section II-A. Consider a directed acyclic graph $G = (V, E)$, with V and E representing the sets of graph vertices and edges respectively. The set of vertices V consists of three subsets A, B, C , representing the initial states, decision states and resulting states respectively, such that $V = A \cup B \cup C$.

For initial state vertices, we consider the numbers of available vehicles at the beginning of epoch t at each cluster. We also subdivide the decision state vertices into the subsets K, L, M of trip, redistribution and idle states respectively, such that $B = K \cup L \cup M$. Finally, for resulting states, we consider the numbers of available vehicles at the beginning of epoch $t + 1$ at each cluster. We associate vertices in each set with the set of road network clusters J such that $|A| = |K| = |L| = |M| = |C| = |J|$. Consequently, the cardinality n of the set V of vertices is $n = |V| = 5|J|$.

A graph edge $(i, j) \in E$ between two vertices $i, j \in V$, represents the change from state i to state j due to allocation decisions. Figure 1 outlines an example of our proposed resource allocation graph with two clusters. We assume vertices in A have directed edges which connect to the vertices in B only in their respective cluster, with a direction from A to B . Consequently, there are 3 edges from vertices in A to vertices in B for each cluster.

We further assume edges between vertices in B and C . Each vertex in K connects to all vertices in C . For redistribution edges starting from vertices in L and terminating to vertices in C , we exclude edges which start and terminate in the same cluster. Finally, for each cluster, we assume an edge from the corresponding cluster vertex in M to the corresponding cluster vertex in C . As such the cardinality m of the set of edges E is $m = |E| = 3|J| + |J|^2 + |J|(|J| - 1) + |J| = |J|(2|J| + 3)$.

To assist our minimum cost flow formulation, we introduce the following functions on E : a lower bound $l_{ij} \geq 0$, a capacity $u_{ij} \geq l_{ij}$ and a cost c_{ij} for each $(i, j) \in E$. Furthermore, we introduce the balance vector function $b : V \rightarrow \mathbb{Z}$ which associates integer numbers with each vertex in V . We assume the following holds:

$$\sum_{v \in V} b(v) = 0 \quad (5)$$

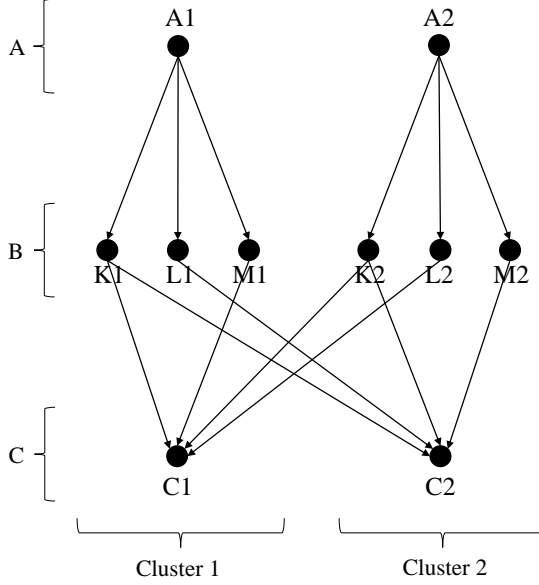


Fig. 1. Example of the proposed resource allocation graph with 2 clusters.

We denote the flow in graph G as a function $x : E \rightarrow \mathbb{Z}^{\geq 0}$ on the edge set of G , such that the value of the flow on edge (i, j) is x_{ij} . The balance vector function $b(v)$ for each $v \in V$ is the difference between the flow in edges of out-degree of v and the flow in edges of in-degree of v . As such, the balance vector b is the following function on the vertices:

$$b(j) = \sum_{i:j \in E} x_{ji} - \sum_{i:j \in E} x_{ij} \quad \forall j \in V \quad (6)$$

We classify vertices with $b(v) > 0$ as source vertices, whereas vertices with $b(v) < 0$ are sink vertices. Otherwise, if a vertex has $b(v) = 0$ we call that vertex balanced. Consequently, a flow x in G is feasible if $l_{ij} \leq x_{ij} \leq u_{ij}$ for all $(i, j) \in E$ and equations (5) and (6) hold for all vertices $v \in V$. Considering our resource allocation problem introduced in Section II-A, we can regard the vertices $v \in A$ as source vertices since these constitute the initial states of all vehicles in the fleet. In a similar fashion, the vertices in C can be identified as sinks, however; their balance vectors cannot be defined in advance, as certain demand requirements might lead to violation of (5).

The values of the balance vector function for sink nodes are related to the demand for trips towards each cluster in the road network. As the minimum cost formulation for solving the resource allocation problem would adhere that a feasible flow satisfies equations (5) and (6), we transform our graph from a multi-source, multi-sink to a multi-source, single-sink one. To do so, we introduce the set of vertices D , for which $|D| = |J|$ such that there is one vertex from set D in each cluster. We also introduce sink vertex t for which $t \cap J = \emptyset$. Vertices in D denote demand satisfiability for the subsequent period. Consequently we have $V \leftarrow V \cup (D \cup t)$.

Vertices from C are connected with edges to vertices in D in each cluster, to denote that vehicles which terminate their tasks or are idle in a cluster during a time epoch, could be available

if needed in the same cluster for the subsequent period. Furthermore, to account for excess vehicles for subsequent demand, we also consider directed edges from all vertices in C to the sink vertex t . We transfer the flow from vertices in D to the sink vertex t by including additional directed edges between them.

Edges starting from vertex sets K to C in each cluster as shown in Figure 1 represent trip edges. If we focus on an individual cluster, the vehicle flow through these edges originates from the same cluster and aims to satisfy the demand for the commencing period. However, depending on geographical proximity, redistributing vehicles from other areas might arrive in the cluster before the end of the commencing period. As a consequence, redistributing vehicles could be exposed to a portion of the demand originating from the cluster during the commencing period.

The above description implies that within a period, in each cluster, there can be variable supply levels exposed to variable demand portions due to the mixing of redistributing vehicles from different clusters. This behaviour is captured in the formulation of the rebalancing problem in [21]. To account for the intra-period redistribution mixing, we introduce additional sets of vertices and edges to the network described in Figure 1 between the vertex sets of B and C . Specifically, in each cluster, we add vertices representing the arrival of vehicle flow from redistributing vertices L from other clusters. As a consequence, we add $|J| - 1$ vertices in each cluster. These additional vertices are extensions to the vertex subset K since they are trip vertices.

We then connect each additional edge in K with a redistribution vertex in L from other clusters, resulting in $|J|(|J| - 1)$ additional edges. We also connect each additional edge in K with all vertices in C , resulting in $J^2(|J| - 1)$ additional edges. Furthermore, to model the vehicle mixing with vehicles already in each cluster, we need to add edges from the original vertices in K , to the additional vertices in K . To do so, we identify the sequence of vehicle mixing using a sorted list of the arrival times in each cluster.

For convenience, in each cluster i in J , we denote original vertices in K as K_i . As the arrival of vehicles from other clusters has a cumulative effect on the supply in each cluster, we denote the additional vertices in K using the sequence of arrivals. For example, if vehicles from L_j arrive in cluster i before vehicles from L_k for i, j, k in J , we denote the vertices corresponding to the mixing of vehicles as K_{ij} and K_{ijk} , for redistribution occurring from clusters j and k respectively. Finally, to complete the mixing, in each cluster, we introduce $|J| - 1$ edges between the intra-cluster vertices in K according to the sequence of arrivals. Revisiting the above example, in cluster i , directed edges are introduced from K_i to K_{ij} and from K_{ij} to K_{ijk} . An outline of the transformed graph is shown in Figure 2. As such, the following equations hold:

$$b(v) > 0 \quad \forall v \in A \quad (7)$$

$$b(v) = 0 \quad \forall v \in B \cup C \cup D \quad (8)$$

$$b(t) < 0 \quad (9)$$

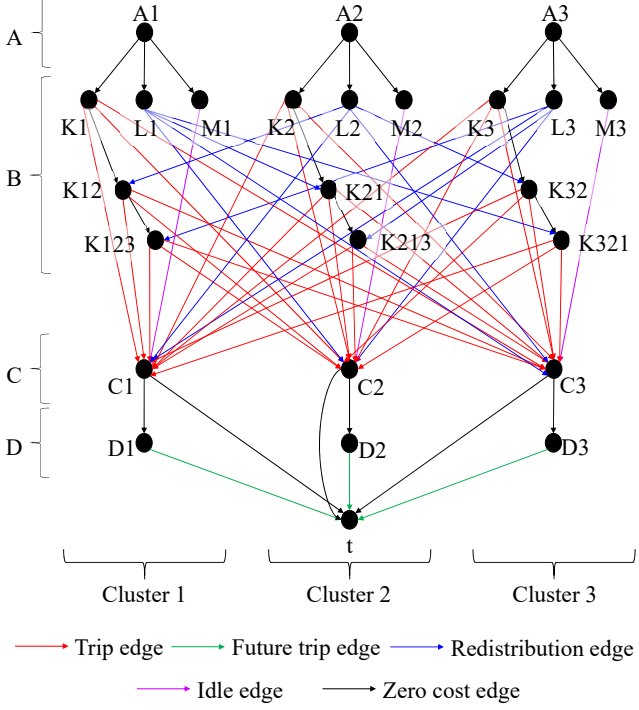


Fig. 2. Example of the transformed single source/sink resource allocation graph with 3 clusters.

To assist our notation, we define a function $n : V \rightarrow J$, which maps vertices of the resource allocation network to clusters in J . Furthermore, to simplify set notation for edges, we define the edge sets $\mathcal{A}, \mathcal{B}, \mathcal{C}, \mathcal{D}, \mathcal{E} \in E$. These edge sets represent the trip, future trip, redistribution, idle and zero cost edges respectively, as described in Figure 2. As such, we define the cost functions for the edges in the graph as follows:

$$c_{ij}(x_{ij}) = h_{ij}(x_{ij}) \quad \forall(i, j) \in \mathcal{A} \quad (10)$$

$$c_{ij}(x_{ij}) = r_{n(i)n(j)}^1 C_M x_{ij} \quad \forall(i, j) \in \mathcal{C} \quad (11)$$

$$c_{ij}(x_{ij}) = C_I x_{ij} \quad \forall(i, j) \in \mathcal{D} \quad (12)$$

$$c_{ij}(x_{ij}) = f_{ij}(x_{ij}) \quad \forall(i, j) \in \mathcal{B} \quad (13)$$

$$c_{ij}(x_{ij}) = 0 \quad \forall(i, j) \in \mathcal{E} \quad (14)$$

Equations (10)-(12) define the cost functions for edges directed from decision state vertices B to vertices in C . Equation (10) denotes the profit⁵ from potential trip allocations with a supply of x_{ij} using function $h_{ij}(x_{ij})$. Parameter $r_{n(i)n(j)}^1$ is the average travel time between the clusters $n(i)$ and $n(j)$ of vertices i and j at the initial epoch as introduced in equation (1), and C_M is the cost of a moving vehicle per time. Consequently, equation (11) defines the cost of redistribution for vehicles. Equation (12) defines the cost of idle vehicles, with C_I to denote the cost of an idle vehicle per period.

Equation (13) defines the potential profit for vehicles available in a cluster in the subsequent period using function

⁵Any profit has a negative sign as we subtract the revenues from the costs to identify it.

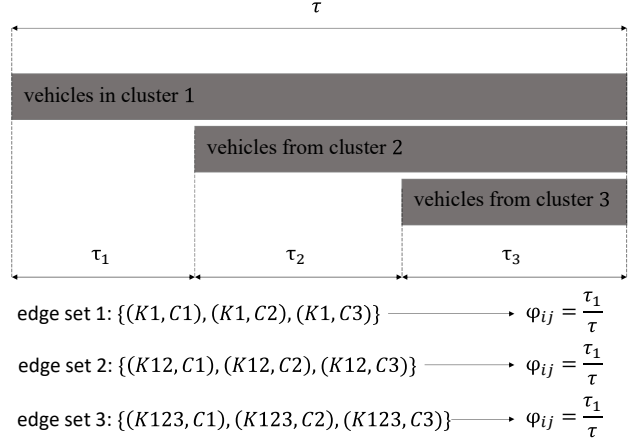


Fig. 3. Example of how the demand factors ϕ are calculated in cluster 1 of an instance with 3 clusters and decision epoch of length τ .

$f_{ij}(x_{ij})$. As such, it guides vehicle redistribution and idle vehicle strategies. Finally, we set the cost to zero for the remaining edges.

Functions $h_{ij}(x_{ij})$ and $f_{ij}(x_{ij})$ in equations (10) and (13) are outlined in the following equations:

$$h_{ij}(x_{ij}) = -\phi_{ij} N_{n(i)n(j)}^1(x_{ij}) p r_{n(i)n(j)}^1 + C_M r_{n(i)n(j)}^1 x_{ij} \quad \forall(i, j) \in \mathcal{A} \quad (15)$$

$$f_{ij}(x_{ij}) = \sum_{m \in J} \left(-N_{n(i)m}^2 \left(\frac{x_{ij}}{|J|} \right) p r_{n(i)m}^2 + C_M r_{n(i)m}^2 x_{ij} \right) \quad \forall(i, j) \in \mathcal{B} \quad (16)$$

As observed in equations (15) and (16), both functions utilise $N_{ij}^t(x)$, which refers to the number of travellers choosing the service given a supply of vehicles x introduced in equation (4). Parameter p is the revenue per time for each vehicle as in equation (1), r_{ij}^t is the travel time between clusters i and j during epoch t as in equations (1) and (11). To accommodate vehicle mixing from redistribution, we factor the number of travellers $N_{ij}^t(x)$ in equation (15) by a factor $\phi_{ij} \in [0, 1]$ according to the arrival sequence of redistributing vehicles in each cluster. A visual demonstration of how the demand factor ϕ_{ij} is calculated for each edge in \mathcal{A} in a cluster is highlighted in Figure 3.

We further define the lower bounds of all vertices to zero and unbounded edge capacities as follows:

$$l_{ij} = 0 \quad \forall(i, j) \in E \quad (17)$$

$$u_{ij} = \infty \quad \forall(i, j) \in E \quad (18)$$

We also define the balance vectors for the source and sink vertices s and t as follows:

$$b(i) = S_i \quad \forall i \in A \quad (19)$$

$$b(t) = - \sum_{v \in A} b(v) = - \sum_{i \in A} S_i \quad (20)$$

Parameter S_i in (19) and (20) denotes the available vehicles S_i in cluster $n(i)$ at the start of the current period.

As such, the resource allocation problem introduced in section II-A can be solved using the following nonlinear minimum cost flow optimization problem:

Model 1:

$$\text{minimize} \quad \sum_{(ij) \in E} c_{ij}(x_{ij}) \quad (21a)$$

subject to

$$x_{ij} \geq l_{ij} \quad \forall (i, j) \in E, \quad (21b)$$

$$x_{ij} \leq u_{ij} \quad \forall (i, j) \in E, \quad (21c)$$

$$b(j) = \sum_{i: j \in E} x_{ji} - \sum_{i: i \in E} x_{ij} \quad \forall j \in V, \quad (21d)$$

$$x_{ij} \in \mathbb{R} \quad \forall (i, j) \in E \quad (21e)$$

Equations (21b)-(21c) ensure the flow of vehicles through each edge (i, j) is within the specified lower and upper bounds respectively, as specified in equations (17) and (18). (21d) is the flow continuity constraint as specified in equation (6).

C. Convex Minimum Cost Flow Transformation

The objective function in (21a) is nonlinear, as a result of the costs for edges in \mathcal{A} and \mathcal{B} . Such cost functions include the term $N_{ij}^t(x)$ introduced in (4), of which its component $q_{ij}^t(x)$ (eq. (3)) and sub-component $w_{ij}^t(x)$ (eq. (2)) are nonlinear. Although $w_{ij}^t(x)$ is by definition a monotonically decreasing convex function within its domain, this is not immediately apparent for (15). Identifying the nature of equation (15) is paramount for the choice of a solution method for *Model 1*⁶.

To assist our analysis, we assume there is only one alternative ride-sourcing option which offers identical pricing rates and travel times, with a fixed wait time \bar{w} . We also assume that travellers quantify their utility of choosing the alternative option using the same utility function as the one introduced in (1). As such, we differentiate the quality of each option using the wait time equation in (2). We expect that the ride-sourcing platform prices its rides at a rate higher than its cost per time, such that $p > C_M$. We finally assume Z_{ij}^t is large enough to justify the cost of redistribution. For notation convenience, we omit any index notation i, j, t in the proof of the following theorem.

Theorem 1. $h_{ij}(x_{ij})$ has an absolute minimum point in $x_{ij} \in [0, \infty]$.

Proof. We first consider the limit of $h(x)$ (eq. (15)) as $x \rightarrow \infty$. We note that $\lim_{x \rightarrow \infty} w(x) = 0$, therefore, $\lim_{x \rightarrow \infty} u(x)$ is equal to some constant value $-r(\bar{v} + p)$. Consequently for $x \rightarrow \infty$, $q(x)$ converges to some finite maximum probability

⁶Classifying equation (15) would suffice because (16) is a linear sum of equation (15) instances.

p_{max} . Since the upper bound of $q(x)$ is 1, $\lim_{x \rightarrow \infty} N(x) = Z$. It is therefore straightforward to deduce the following limit:

$$\lim_{x \rightarrow \infty} h(x) = \infty \quad (22)$$

We now consider the limit of $h(x)$ for $x \rightarrow 0^+$. For a large Z , $\lim_{x \rightarrow 0^+} w(x) = \alpha Z$, $\lim_{x \rightarrow 0^+} u(x) = -\bar{u}(\alpha Z + r) - pr$. Due to the exponential nature of $q(x)$, for small values of x (i.e. $x = 1$ for large Z), we have that $\lim_{x \rightarrow 0^+} q(x) = 0$ and consequently $\lim_{x \rightarrow 0^+} N(x) = 0$. Therefore we arrive to the following result:

$$\lim_{x \rightarrow 0^+} h(x) = 0^+ \quad (23)$$

Let us now explore the case of $q(x) = 0.5$. For $q(x) = 0.5$, $w(x) = \bar{w}$, therefore by rearranging the terms of $w(x)$, for $w(x) = \bar{w}$, we have that $x = \frac{\alpha}{\bar{w}}Z - 1$. Since $q(x) = 0.5$, equation (15) results to $h(x) = -0.5Zpr + C_{Mrx}$. Substituting x with $\frac{\alpha}{\bar{w}}Z - 1$, and simplifying we have the following equation:

$$h(x) = r \left(-0.5Zp + C_M \left(\frac{\alpha}{\bar{w}}Z - 1 \right) \right) \quad (24)$$

We know that the fleet operator chooses p such that $p > C_M$. Therefore, by appropriately choosing the cluster area sizes, we can scale α , such that $\alpha < \bar{w}$ and $-0.5Z > \frac{C_M}{p}(\frac{\alpha}{\bar{w}}Z - 1)$. Thus, by implementing the above inequalities, for $q(x) = 0.5$, the following relationship holds:

$$h(x) < 0 \quad \forall x \in \mathbb{R}^+ | q(x) = 0.5 \wedge \frac{C_M \alpha}{p \bar{w}} \leq 0.5 \quad (25)$$

Using equations (22) and (23), and by showing that $h(x)$ is negative for some $x \in \mathbb{R}^+$, we conclude that $h(x)$ has an absolute minimum point in $x \in [0, \infty]$. \square

Corollary 1. $h_{ij}(x_{ij})$ is convex for some domain $x_{ij} \in [x'_{ij}, x^*_{ij}]$. Where $h_{ij}(x^*_{ij})$ is the absolute minimum value of $h_{ij}(x_{ij})$ for $x_{ij} \in \mathbb{R}^+$ and x'_{ij} is the largest value of x_{ij} such that $h(x'_{ij})$ is a non-stationary inflection point and $x'_{ij} < x^*_{ij}$.

Our aim is to identify and utilize the convexity of the domain $[x'_{ij}, x^*_{ij}]$ of each non-linear edge cost function to solve *Model 1* as a convex minimum cost flow problem. In line with convexity, we replace the upper bounds u_{ij} of each non-linear edge (i, j) to the absolute minimum value x^*_{ij} . Therefore additional to equation (18), we introduce the following:

$$u_{ij} = x^*_{ij} \quad \forall (i, j) \in \mathcal{A} \cup \mathcal{B} \quad (26)$$

In a similar fashion, setting the lower bound l_{ij} of any non-linear edge (i, j) to the inflection point x'_{ij} , would restrain our non-linear cost functions to the convex domain. Nonetheless, we refrain setting lower bounds to our problem to avoid potential infeasibility of *Model 1*. Instead, we split each non-linear cost function to a piece-wise one, with a linear part between $[0, x'_{ij}]$, and non-linear convex part between $[x'_{ij}, x^*_{ij}]$. We linearise $h_{ij}(x_{ij})$ between $[0, x'_{ij}]$ to avoid any concave parts of the cost misguiding our solution algorithm (Section II-D) towards non-optimal solutions.

As we will see in the next section (Section II-D), our proposed solution algorithm identifies optimal solutions of convex functions by incrementally moving from higher absolute values of the cost derivative $\frac{dh_{ij}(x_{ij})}{dx_{ij}}$ towards values where the derivative approaches zero ($\frac{dh_{ij}(x_{ij}^*)}{dx_{ij}} = 0$). Consequently, we set the equation of the linearised part $h_{ij}^L(x_{ij})$ between $[0, x_{ij}']$ for $h_{ij}(x_{ij})$ to the equation of the tangent of $h_{ij}(x_{ij})$ at x_{ij}' follows:

$$h_{ij}^L(x_{ij}) = \frac{dh_{ij}(x_{ij}')}{dx_{ij}}x_{ij} - \frac{dh_{ij}(x_{ij}')}{dx_{ij}}x_{ij}' + h_{ij}(x_{ij}') \quad (27)$$

Similarly, by performing the same procedure for $f_{ij}(x_{ij})$ in equation (16), the linearised part of the cost has the following form:

$$f_{ij}^L(x_{ij}) = \frac{df_{ij}(x_{ij}')}{dx_{ij}}x_{ij} - \frac{df_{ij}(x_{ij}')}{dx_{ij}}x_{ij}' + f_{ij}(x_{ij}') \quad (28)$$

We thereby introduce the following convex cost functions to replace equations (10) and (13) with equations (29) and (30) respectively:

$$c_{ij}(x_{ij}) = h_{ij}^C(x_{ij}) \quad \forall (i, j) \in \mathcal{A} \quad (29)$$

$$c_{ij}(x_{ij}) = f_{ij}^C(x_{ij}) \quad \forall (i, j) \in \mathcal{B} \quad (30)$$

The functions $h_{ij}^C(x_{ij})$ and $f_{ij}^C(x_{ij})$ in equations (29) and (30) respectively have the following form:

$$h_{ij}^C(x_{ij}) = \begin{cases} h_{ij}^L(x_{ij}) & x_{ij} \leq x_{ij}' \\ h_{ij}(x_{ij}) & x_{ij} > x_{ij}' \end{cases} \quad (31)$$

$$f_{ij}^C(x_{ij}) = \begin{cases} f_{ij}^L(x_{ij}) & x_{ij} \leq x_{ij}' \\ f_{ij}(x_{ij}) & x_{ij} > x_{ij}' \end{cases} \quad (32)$$

As such, by replacing equations (10) and (13) with equations (29) and (30) respectively and adapting the upper bounds of equation (26) for non-linear edges, *Model 1* becomes a Convex Minimum Cost Flow (CMCF) optimization problem.

D. Edge-Splitting Pseudo-Polynomial Algorithm

It was previously mentioned that it is possible to transform our vehicle redistribution problem into a CMCF problem. The flow x_{ij} is a discrete quantity in our model as it considers the count of vehicles in each link (i, j) . Linear Minimum cost flow models adhere to the following theorem, as stated in [23]:

Theorem 2. (Integrality Theorem) *If the capacities of all edges and the balance values of all the nodes are integer, the linear minimum cost flow problem always has an integer optimal flow.*

For proof of the above theorem, we refer readers to [23]. We thus deduce by restricting the parameters of the problem to integers (capacities and balance vectors), we can solve the linear minimum cost flow problem in polynomial time. We aim to exploit the integrality theorem, using an appropriate linearisation technique, to solve the CMCF problem transformation of *Model 1* in polynomial time.

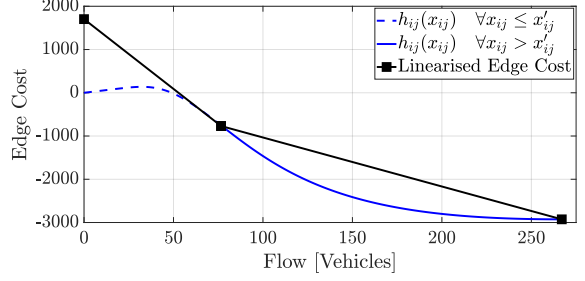


Fig. 4. Cost Function Variation for Edges $(i, j) \in \mathcal{A}$.

The CMCF problem has been previously tackled efficiently in the literature. [24] initially proposed an extension of the scaling method for linear minimum cost flows presented in [25], for convex cost flows with quadratic functions. At a subsequent stage, [26] and [27] separately conducted studies on solving minimum cost flows with general convex objectives. A variant of the algorithm proposed by [26], and along the lines of [27], is featured in [23]. [28] proposed polynomial algorithms for solving the CMCF problem in circles, lines or trees. The problem of quadratic CMCF was also tackled more recently in [29], using an enhanced version of [26], utilizing the technique for linear minimum cost flows proposed in [30].

A consistent assumption of the studies which efficiently address the CMCF problem is that the edge costs are non-negative. Nonetheless, as we have seen in sections II-B and II-C, the non-linear cost functions of *Model 1* can have negative values. The notion of negative costs (i.e. profit), implies that in an optimal solution of *Model 1*, there would be edges with negative costs. As such, we refrain from using the above algorithms, and instead, we incorporate a modified version of the pseudo-polynomial algorithm for CMCF presented in [23].

Our algorithm applies piece-wise linearisation by introducing parallel linear edges for each non-linear edge in the network. To limit the amount of additional parallel edges in the network, we start the algorithm with only two parallel edges for each non-linear edge (i, j) . As observed in equations (31) and (32), $h_{ij}^C(x_{ij})$ and $f_{ij}^C(x_{ij})$ are partly linearized (i.e. for $x \leq x_{ij}'$). Consequently, by replacing $h_{ij}(x_{ij})$ and $f_{ij}(x_{ij})$ with their linearised versions between x_{ij}' and x_{ij}^* , we initiate our algorithm with two parallel linear edges for each non-linear edge of *Model 1*. Figures⁷ 4 and 5 outline the initial linearisation of costs for non-linear edges $(i, j) \in \mathcal{A}$ and $(i, j) \in \mathcal{B}$ respectively.

As observed in figures 4 and 5, due to convexity, the slope of each parallel linear edge from left to right gradually increases, from a minimum negative value to zero, as we move from $x_{ij} = 0$ to $x_{ij} = x_{ij}^*$. Consequently, per unit flow is more expensive through the parallel linear edge corresponding to the non-linear section for $x_{ij} > x_{ij}'$. As such, assuming both parallel edges have residual capacity, flow through parallel edges with smaller slope is always prioritised over edges with

⁷For figures 4 and 5 we used the following parameters: $\bar{v} = 0.3$, $\alpha = 2$, $\bar{w} = 5$, $p = 1$, $C_M = 0.3$.

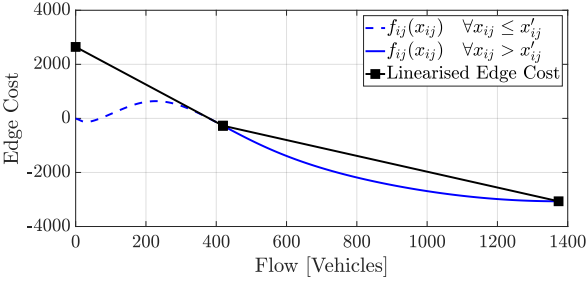


Fig. 5. Cost Function Variation for Edges $(i, j) \in \mathcal{B}$.

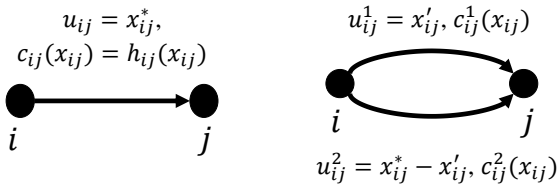


Fig. 6. Linear transformation of a non-linear edge (i, j) to linear edges $(i, j)^1$ and $(i, j)^2$ with resulting linear costs c_{ij}^1 and c_{ij}^2 respectively.

larger slope value (i.e. closer to zero). This observation is described as the property of contiguity in [23].

Utilizing contiguity, for each parallel linear edge, we set the upper bound (capacity), to the difference between the right and left flow boundaries of the linearised edge, while maintaining zero lower bounds. Consequently, for our initial linearisation configuration, the upper bounds will be $u_{ij}^1 = x'_{ij} - 0$ and $u_{ij}^2 = x_{ij}^* - x'_{ij}$ from left to right respectively, as observed in figures 4 and 5. Since we initiate our algorithm with two parallel linear edges per non-linear edge, we denote their linear cost functions as c_{ij}^1 and c_{ij}^2 for edges corresponding to $x \leq x'_{ij}$ and $x_{ij} > x'_{ij}$ respectively. We show the transformation of each non-linear edge to a pair of linearised ones in figure 6.

To maintain the validity of Theorem 2, we consider integer versions of x'_{ij} and x_{ij}^* , such that the resulting capacities u_{ij}^1 and u_{ij}^2 are also integers. Furthermore, to identify point x'_{ij} for each non-linear edge in *Model 1*, we approximate the first and second derivatives of the non-linear cost using the forward and central difference formulas respectively.

We introduce function $P(i, j)$ which identifies the set of parallel edges between any pair of vertices $i, j \in V$. We also refer to the linearised version of $G = (V, E)$ as $G_L = (V, E_L)$. Our non-linear edge linearisation of *Model 1* up to this point can be described via the following formulation:

Model 2:

$$\text{minimize} \quad \sum_{(ij) \in E} \sum_{k=1}^{P(i,j)} c_{ij}^k(x_{ij}^k) \quad (33a)$$

subject to

$$x_{ij}^k \geq l_{ij}^k \quad \forall (i, j) \in E, \forall k \in P(i, j), \quad (33b)$$

$$x_{ij}^k \leq u_{ij}^k \quad \forall (i, j) \in E, \forall k \in P(i, j), \quad (33c)$$

$$b(j) = \sum_{i:ji \in E} \sum_{k=1}^{P(j,i)} x_{ji}^k - \sum_{i:ij \in E} \sum_{k=1}^{P(i,j)} x_{ij}^k \quad \forall j \in V, \quad (33d)$$

$$x_{ij}^k \in \mathbb{R} \quad \forall (i, j) \in E, \forall k \in P(i, j) \quad (33e)$$

A high level structure of our CMCF algorithm is outlined in Algorithm 1. Algorithm 1 utilizes graphs G and G_L , and the structure of *Model 2* to identify the set of minimum cost flows F , such that $x_{ij}^k \in F$, with $(i, j)^k \in E_L$. Algorithm 1 incorporates an iterative procedure to arrive at the optimal solution for the CMCF of graph G .

Algorithm 1 CMCF Edge-Splitting Algorithm

```

1: Inputs: Model 2, graph  $G_L$  and graph  $G$ 
2:  $OPT = \text{false}$ 
3: while  $OPT = \text{false}$  do
4:    $F \leftarrow \emptyset$ 
5:    $F = \text{NetworkSimplex}(F, G_L, \text{Model 2})$ 
6:    $U = \text{SplittableEdges}(F, G_L)$ 
7:   if  $U = \emptyset$  then
8:      $OPT = \text{true}$ 
9:   else
10:    for  $(i, j)^k \in U$  do
11:       $G_L = \text{Split}(G, G_L, (i, j)^k)$ 
12:    end for
13:   end if
14: end while
15: Output: Flow  $F$ 

```

To facilitate our edge-splitting algorithm, we define the boolean variable OPT with the default value set to false, which signals the algorithm to stop if an optimal solution is found during an iteration (i.e. if OPT is true). At the beginning of each iteration, we use the network simplex algorithm [23] to solve the minimum cost flow problem and obtain a set F of flows x_{ij}^k . We thereby screen through flows $x_{ij}^k \in F$ using the function $\text{SplittableEdges}(F, G_L)$, to identify the set U of linearised parallel edges which are subject to further splitting. If U is an empty set, the set F of flows x_{ij}^k is an optimal solution to the CMCF version of *Model 1*. Otherwise, we proceed with splitting each edge $(i, j)^k \in U$ using the routine $\text{Split}(G, G_L, (i, j)^k)$, which updates the linearised graph G_L and move to the next iteration.

We use the function $\text{NetworkSimplex}(F, G_L, \text{Model 2})$ to denote the procedure of solving *Model 2* using network simplex and populating set F . We omit presentation of the network simplex algorithm as it is well known in the literature. The routine followed for the $\text{SplittableEdges}(F, G_L)$ function is outlined in Algorithm 2. As observed in Algorithm 2, we investigate the flow of each parallel edge $(i, j)^k$ of graph G_L which exists in the convex domain of edge (i, j) of graph G (i.e. $k > 1$). If the edge $(i, j)^k$ is the first edge in (i, j) which is not at capacity and can be divided, we add edge $(i, j)^k$ to the set U .

The $\text{Split}(G, G_L, (i, j)^k)$ function used in Algorithm 1 is outlined in Algorithm 3. Initially, we identify the corresponding upper (x_U) and lower (x_L) flow values of edge $(i, j)^k$ in the convex domain of edge (i, j) . Since the flow F is

Algorithm 2 SplittableEdges Function

```

1: Inputs: Set  $F$  of flows  $x_{ij}^k$ , graph  $G_L$ 
2:  $U \leftarrow \emptyset$ 
3: for  $(i, j) \in ((K \times C) \cup (D \times t))$  do
4:   for  $k \in P(i, j) \setminus k = 1$  do
5:     if  $(l_{ij}^k \leq x_{ij}^k < u_{ij}^k) \cup (x_{ij}^{k-1} = u_{ij}^{k-1})$  then
6:       if  $(u_{ij}^k > 1)$  then
7:          $U \leftarrow U \cup (i, k)^k$ 
8:       end if
9:     end if
10:   end for
11: end for
12: Output: Set  $U$  of splittable edges

```

contiguous, we can find x_U and x_L by finding the total flow in (i, j) , and the total flow in (i, j) excluding x_{ij}^k respectively. We then identify the split point x_S as the midpoint⁸ of x_U and x_L . We thus remove the edge $(i, j)^k$ and append $P(i, j)$ with the indices of the two new parallel edges to be added. For each new parallel edge, we find its upper and lower bound, as well as its cost function in a similar fashion as described earlier in the construction of G_L before initialising Algorithm 1. We conclude the split function by adding the two new parallel edges in E_L and returning the updated graph G_L .

Algorithm 3 Split Function

```

1: Inputs: Graph  $G$ , graph  $G_L$  and edge  $(i, j)^k$ 
2:  $x_U = \sum_{n \in P(i, j)} x_{ij}^n$ 
3:  $x_L = \sum_{n \in P(i, j) \setminus n=k} x_{ij}^n$ 
4:  $x_S = \lceil \frac{x_{ij}^U + x_{ij}^L}{2} \rceil$ 
5:  $E_L \leftarrow E_L \setminus (i, j)^k$ 
6:  $n = \max(P(i, j))$ 
7:  $P(i, j) \leftarrow P(i, j) \cup (n+1) \cup (n+2)$ 
8:  $u_{ij}^{n+1} = x_S - x_L$ 
9:  $u_{ij}^{n+2} = x_U - x_S$ 
10:  $l_{ij}^{n+1} = 0$ 
11:  $l_{ij}^{n+2} = 0$ 
12: Define  $c_{ij}^{n+1}(x)$  by finding the linear equation between points  $[x_L, c_{ij}(x_L)]$  and  $[x_S, c_{ij}(x_S)]$ .
13: Define  $c_{ij}^{n+2}(x)$  by finding the linear equation between points  $[x_S, c_{ij}(x_S)]$  and  $[x_U, c_{ij}(x_U)]$ .
14:  $E_L \leftarrow E_L \cup (i, j)^{n+1} \cup (i, j)^{n+2}$ 
15: Output: Updated linearised graph  $G_L$ 

```

The rationale behind our solution method, as described in Algorithms 1-3, is that we keep splitting linearised edges in the convex domain until we satisfy some optimality conditions. Specifically, we obtain the optimal solution when all the flows in each of the linearised edges in this domain are either zero or equal to the upper bound, and no further splitting can induce incremental cost savings.

If the total input flow (i.e. $\sum_{i \in A} S_i$) is large enough, Algorithm 1 allocates the upper bound flow in each of the non-linear edges of G due to their negative costs (profitable

edges). The case described above would terminate after the first iteration with the optimal solution of the CMCF version of *Model 1*. Otherwise, for each non-linear edge, the first parallel edge which is not at capacity is split into two parts. For any split edge, due to convexity, the flow in the next iteration would always be confined within the resulting pair of parallel edges.

As a result of the above description, Algorithm 1 terminates when for each non-linear edge, the splitting procedure produces parallel edges of unit capacity (i.e. $u_{ij}^k = 1$). Consequently, the number of iterations is logarithmic and relates to the maximum interval $x_{ij}^* - x_{ij}'$ out of all the non-linear edges. If we denote this maximum interval as Δ , we need to solve the minimum cost flow problem $\log_2(\Delta)$ times, adding at most $|J|^3 + |J|$ parallel edges to G_L at each iteration.

We can express the cardinality m of the set of edges E in terms of $|J|$; hence each network simplex run is polynomially bounded by the number of variables of the original problem. However, we cannot express Δ by the number of variables in the network G . Consequently, Algorithm 1 runs in pseudo-polynomial time. Nonetheless, even in extreme practical cases $\log_2(\Delta)$ is a small number (i.e. for $\Delta = 10000$, $\log_2(\Delta) \approx 13$), hence our algorithm can be applied in practical implementations.

III. DISCUSSION

We tested the effectiveness of our redistribution algorithm in a simulated ride-sourcing fleet operator using an agent-based modelling framework with a first-in-first-out (FIFO) customer assignment policy. We implemented our algorithmic methodology in Python, which served as the fleet management logic in our agent-based model and tested on a workstation with an Intel i7-4790 CPU (3.6GHz) and 8GB RAM. We used the IBM Cplex solver to obtain network simplex solutions for *Model 2*.

We selected the area of Manhattan, NYC to apply a case study of the algorithm due to the comprehensive trip data-set available in [31] which served as our demand input. Travel times in the network were calculated using the OSMnx library [32]. By assuming a small proportion of traffic attributes to ride-sourcing, we omitted endogenous congestion in our agent-based model. Nonetheless, we accounted for exogenous congestion by applying a 20% penalty to the free-flow speeds in residential and motorway link segments, and 40% elsewhere during peak hours.

Using the data-set in [31], we created typical demand profiles for weekdays in Manhattan, NYC. By setting the length τ of each optimization period (time-horizon) to 30 minutes, we used our vehicle redistribution algorithm in our agent-based model every 30 minutes from 07:00 am to 12:00 am. We tested our algorithm using different fleet sizes from 2500 to 15000 vehicles. K-means clustering was used to split the road-network into five clusters, as shown in figure 7.

The values of α and \bar{w} were set to 2 and 5 (minutes) respectively, after calibration. For this study, we used UK⁹ estimates of the value of time \bar{v} and vehicle moving costs C_M from [33]. Consequently, the average value of time \bar{v} was

⁸ $\lceil X \rceil$ denotes the ceiling function.

⁹Data on values of time for New York were not available.

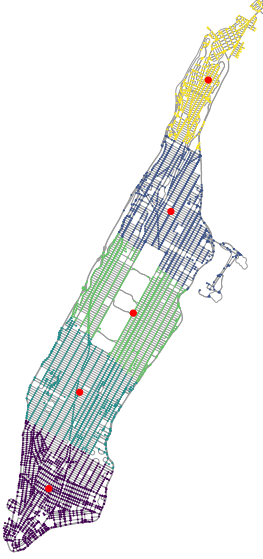


Fig. 7. Cluster split for the road-network of Manhattan, NY. Red dots represent cluster centroid road-nodes.

set to 17.69 GBP/hour and the vehicle moving cost C_M was set to the conservative estimate of 12.96 GBP/hour to reflect current driver valuations¹⁰. The idle vehicle cost C_I was set to 5 GBP to account for mixed roaming and parking costs with 30 minutes, whereas the price per minute for a ride p was set to 1.00 GBP/min to reflect previous research on AV pricing [5].

To benchmark the performance of our algorithm, we test it against the case of no redistribution and also against a redistribution method from the state-of-the-art which does not assume any supply-demand elasticity or underlying market structure, namely the rebalancing model by Wallar et al. [21]. For the model in [21] we use the same decision and rebalancing window of 30 minutes as in our algorithm.

Our algorithm performs allocations based on demand expectations for two subsequent periods (Z_{ij}^1 and Z_{ij}^2). Since the application of predictive algorithms is beyond the scope of this paper, we assumed that the platform has complete knowledge of the demand in the two subsequent periods for each cluster when applying our algorithm and the model in [21]. In reality, fleet operators have access to vast amounts of data; thus, we expect that predictive algorithms can provide demand estimates at an acceptable accuracy level.

As observed in figure 8, vehicle redistribution via our algorithm can reduce the average customer wait time up to almost 50% when compared to no redistribution. Comparing the results of our algorithm with the method proposed in [21], we see that our algorithm always achieves longer wait times even though the difference is not marginal. Nonetheless, as outlined in figure 9, we observe that our algorithm performs better than the method in [21] when comparing the number of aborted customers for fleet sizes from 2500 to 7500.

¹⁰Autonomous vehicles are expected to cost less per time when compared to conventional vehicles

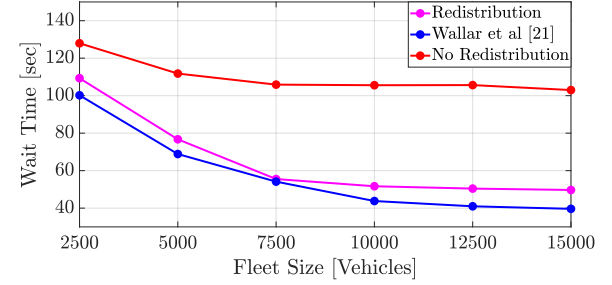


Fig. 8. Average wait time of customers for different fleet sizes and redistribution strategies.

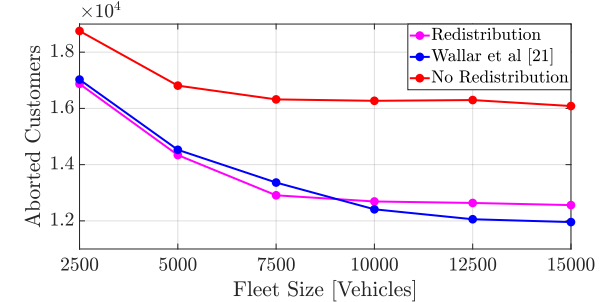


Fig. 9. Number of customers aborting for different fleet sizes and redistribution strategies.

Furthermore, both algorithms achieve a sizeable decrease in the count of aborted customers when compared to the case of no redistribution.

As noted in equation 3, we used a nested-logit model to identify traveller choices. To simplify the problem, we assumed a demand catchment of travellers who are only interested in ride-sourcing and assumed only one competitor. Furthermore, we assumed demand homogeneity (i.e. nested-logit parameters are drawn from the same probability distribution), although, in reality, the demand might follow a parametric distribution. Consequently, the value of redistribution is influenced by population characteristics.

In our simulated scenarios, we found that our redistribution can increase market share by up to 8% when compared to no redistribution, as observed in figure 10. We also observe that although our method always achieves longer wait times than the rebalancing method in [21], it does manage to gain more market share for fleet sizes between 2500 to 7500. This trend is consistent with the observation in Figure 9 and is a consequence of the market-informed redistribution which our algorithm performs.

To identify whether that increase in market share is profitable, we calculated the utilization of the fleet in vehicles required per hour. We define utilization as the proportion of the total time spent serving clients in an hour, multiplied by the fleet size. As such, we can regard our utilization metric as the number of revenue-generating vehicle hours per hour of the fleet. We observed in figure 11, that utilization follows an almost identical trend as market share.

The increase of market share and vehicle utilization via idle

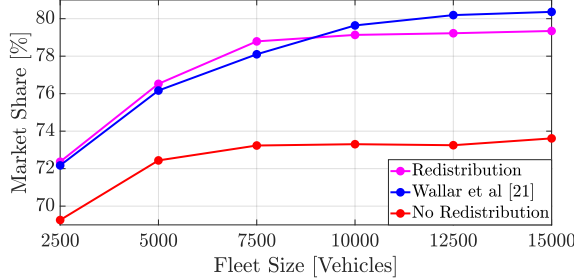


Fig. 10. Market share for different fleet sizes and redistribution strategies.

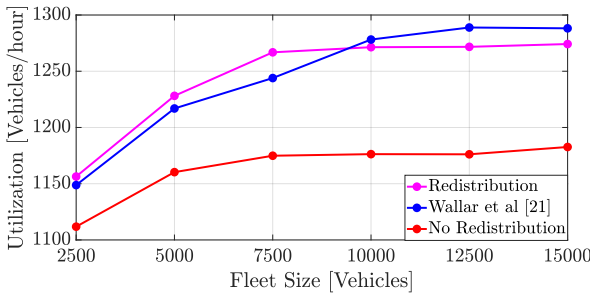


Fig. 11. Fleet utilization for different fleet sizes and redistribution strategies.

vehicle redistribution is achievable with extra vehicle mileage, as observed in figure 12. As the size of the fleets used is small relative to the background traffic, we assumed that extra vehicle mileage due to redistribution has a negligible impact on congestion. As shown in figure 12, our algorithm achieves less vehicle mileage when it is more effective (between 2500 and 7500 vehicles), when compared to the rebalancing method of [21].

IV. CONCLUSION

In this paper, we addressed the problem of vehicle redistribution in autonomous ride-sourcing markets to mediate supply-demand imbalance across a road-network. We used network theory to transform the vehicle redistribution problem into a CMCF problem with negative costs, accounting for customer behaviour under an assumed market structure. Our proposed edge-splitting algorithm solves the CMCF problem

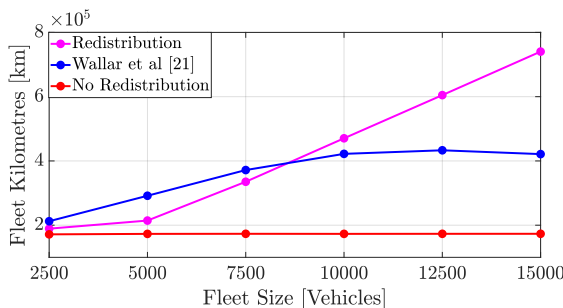


Fig. 12. Total fleet kilometres for different fleet sizes and redistribution strategies.

exactly in pseudo-polynomial time by allocating vehicles to spatio-temporal tasks. We demonstrated the practicability of our redistribution algorithm in an agent-based model simulating ride-sourcing in a large urban setting, such as Manhattan, NYC.

Our suggestions for future research in this area are several. First, we believe that transportation providers should quantify the effects of localised demand choice model structures on the effectiveness of vehicle redistribution. Furthermore, researchers need to investigate the robustness of vehicle redistribution models subject to demand prediction efficacy. The underlying city/road-network structure can influence parameters such as wait time variation and cluster size. As such, studies which focus on the variation of pick-up wait times subject to road network structure could add value to current research. Finally, we note that our model considers an aggregate/discretised spatio-temporal version of the problem, where decision making occurs at a centralised level. We thus believe that thorough scrutiny of both centralised aggregate spatio-temporal models and decentralised (per-vehicle) redistribution models could be useful.

REFERENCES

- [1] T. W. Schneider, “Analyzing 1.1 Billion NYC Taxi and Uber Trips, with a Vengeance,” 2020. [Online]. Available: <https://toddwschneider.com/posts/analyzing-1-1-billion-nyc-taxi-and-uber-trips-with-a-vengeance/>
- [2] M. K. Chen, “Dynamic pricing in a labor market: Surge pricing and flexible work on the uber platform,” in *Proceedings of the 2016 ACM Conference on Economics and Computation*, 2016, pp. 455–455.
- [3] S. Banerjee, C. Riquelme, and R. Johari, “Pricing in ride-share platforms: A queueing-theoretic approach,” Available at SSRN 2568258, 2015.
- [4] H. Qiu, R. Li, and J. Zhao, “Dynamic pricing in shared mobility on demand service,” *arXiv:1802.03559*, 2018.
- [5] R. Karamanis, P. Angeloudis, A. Sivakumar, and M. Stettler, “Dynamic Pricing in One-Sided Autonomous Ride-Sourcing Markets,” in *21st International Conference on Intelligent Transportation Systems (ITSC)*, 2018, pp. 3645–3650.
- [6] M. Dell’Amico, E. Hadjicostantinou, M. Iori, and S. Novellani, “The bike sharing rebalancing problem: Mathematical formulations and benchmark instances,” *Omega*, vol. 45, pp. 7–19, 2014. [Online]. Available: <http://www.sciencedirect.com/science/article/pii/S0305048313001187>
- [7] M. Nourinejad, S. Zhu, S. Bahrami, and M. J. Roorda, “Vehicle relocation and staff rebalancing in one-way carsharing systems,” *Transportation Research Part E: Logistics and Transportation Review*, vol. 81, pp. 98–113, 2015. [Online]. Available: <http://www.sciencedirect.com/science/article/pii/S1366554515001349>
- [8] M. W. Levin, K. M. Kockelman, S. D. Boyles, and T. Li, “A general framework for modeling shared autonomous vehicles with dynamic network-loading and dynamic ride-sharing application,” *Computers, Environment and Urban Systems*, vol. 64, pp. 373–383, 2017.
- [9] H. Yang, S. C. Wong, and K. I. Wong, “Demand-supply equilibrium of taxi services in a network under competition and regulation,” *Transportation Research Part B: Methodological*, vol. 36, no. 9, pp. 799–819, 2002.
- [10] S. Illgen and M. Höck, “Literature review of the vehicle relocation problem in one-way car sharing networks,” *Transportation Research Part B: Methodological*, vol. 120, pp. 193–204, 2019. [Online]. Available: <http://www.sciencedirect.com/science/article/pii/S0191261518300547>
- [11] R. Nair and E. Miller-Hooks, “Fleet management for vehicle sharing operations,” *Transportation Science*, vol. 45, no. 4, pp. 524–540, 2011.
- [12] J. Pfrommer, J. Warrington, G. Schildbach, and M. Morari, “Dynamic vehicle redistribution and online price incentives in shared mobility systems,” *IEEE Transactions on Intelligent Transportation Systems*, vol. 15, no. 4, pp. 1567–1578, 2014.

- [13] D. J. Fagnant and K. M. Kockelman, "The travel and environmental implications of shared autonomous vehicles, using agent-based model scenarios," *Transportation Research Part C: Emerging Technologies*, vol. 40, pp. 1–13, 2014.
- [14] R. Zhang and M. Pavone, "Control of robotic mobility-on-demand systems: a queueing-theoretical perspective," *The International Journal of Robotics Research*, vol. 35, no. 1-3, pp. 186–203, 2016.
- [15] R. Iglesias, F. Rossi, R. Zhang, and M. Pavone, "A bemp network approach to modeling and controlling autonomous mobility-on-demand systems," *The International Journal of Robotics Research*, vol. 38, no. 2-3, pp. 357–374, 2019.
- [16] J. Wen, J. Zhao, and P. Jaillet, "Rebalancing shared mobility-on-demand systems: A reinforcement learning approach," in *2017 IEEE 20th International Conference on Intelligent Transportation Systems (ITSC)*. IEEE, 2017, pp. 220–225.
- [17] K. Lin, R. Zhao, Z. Xu, and J. Zhou, "Efficient large-scale fleet management via multi-agent deep reinforcement learning," in *Proceedings of the 24th ACM SIGKDD International Conference on Knowledge Discovery & Data Mining*, 2018, pp. 1774–1783.
- [18] A. Braverman, J. G. Dai, X. Liu, and L. Ying, "Empty-car routing in ridesharing systems," *Operations Research*, vol. 67, no. 5, pp. 1437–1452, 2019.
- [19] X. Yu, S. Gao, X. Hu, and H. Park, "A Markov decision process approach to vacant taxi routing with e-hailing," *Transportation Research Part B: Methodological*, vol. 121, pp. 114–134, 2019. [Online]. Available: <http://www.sciencedirect.com/science/article/pii/S0191261518303837>
- [20] J. Alonso-Mora, A. Wallar, and D. Rus, "Predictive routing for autonomous mobility-on-demand systems with ride-sharing," in *2017 IEEE/RSJ International Conference on Intelligent Robots and Systems (IROS)*. IEEE, 2017, pp. 3583–3590.
- [21] A. Wallar, M. Van Der Zee, J. Alonso-Mora, and D. Rus, "Vehicle rebalancing for mobility-on-demand systems with ride-sharing," in *2018 IEEE/RSJ International Conference on Intelligent Robots and Systems (IROS)*. IEEE, 2018, pp. 4539–4546.
- [22] R. Iglesias, F. Rossi, K. Wang, D. Hallac, J. Leskovec, and M. Pavone, "Data-driven model predictive control of autonomous mobility-on-demand systems," in *2018 IEEE International Conference on Robotics and Automation (ICRA)*. IEEE, 2018, pp. 1–7.
- [23] R. K. Ahuja, T. L. Magnanti, and J. B. Orlin, *Network Flows Theory, Algorithms and Applications*, P. Janzow and M. Peterson, Eds. New Jersey: Prentice-Hall, 1993, vol. 1.
- [24] M. Minoux, "A polynomial algorithm for minimum quadratic cost flow problems," *European Journal of Operational Research*, vol. 18, no. 3, pp. 377–387, 1984.
- [25] J. Edmonds and R. M. Karp, "Theoretical improvements in algorithmic efficiency for network flow problems," *Journal of the ACM (JACM)*, vol. 19, no. 2, pp. 248–264, 1972.
- [26] M. Minoux, "Solving integer minimum cost flows with separable convex cost objective polynomially," in *Netflow at Pisa*. Springer, 1986, pp. 237–239.
- [27] D. S. Hochbaum and J. G. Shanthikumar, "Convex separable optimization is not much harder than linear optimization," *Journal of the ACM (JACM)*, vol. 37, no. 4, pp. 843–862, 1990.
- [28] J. B. Orlin and B. Vaidyanathan, "Fast algorithms for convex cost flow problems on circles, lines, and trees," *Networks*, vol. 62, no. 4, pp. 288–296, 2013.
- [29] L. A. Vegh, "A Strongly Polynomial Algorithm for a Class of Minimum-Cost Flow Problems with Separable Convex Objectives," *SIAM Journal on Computing*, vol. 45, no. 5, pp. 1729–1761, 2016.
- [30] J. B. Orlin, "A faster strongly polynomial minimum cost flow algorithm," *Operations research*, vol. 41, no. 2, pp. 338–350, 1993.
- [31] TLC, "New York City Taxi Trip Data," New York, NY, 2019. [Online]. Available: <https://www1.nyc.gov/site/tlc/about/tlc-trip-record-data.page>
- [32] G. Boeing, "Osmnx: New methods for acquiring, constructing, analyzing, and visualizing complex street networks," *Computers, Environment and Urban Systems*, vol. 65, pp. 126 – 139, 2017. [Online]. Available: <http://www.sciencedirect.com/science/article/pii/S0198971516303970>
- [33] DfT, "TAG Data Book," DfT, London, UK, Tech. Rep., 2018. [Online]. Available: <https://www.gov.uk/government/publications/tag-data-book>



Renos Karamanis received an M.Eng. degree in Civil and Environmental Engineering from Imperial College London in 2014. From 2014 to 2015 he worked as an engineering consultant for Mott MacDonald, a multi-disciplinary consultancy with headquarters in the United Kingdom.

In 2015 he joined the Centre for Transport Studies in Imperial College London where he is currently a Ph.D. student. His research interests include developing operational research methods to improve the efficiency of pricing, assignment and resource allocation of autonomous ride-sourcing fleets, and simulation modelling of ride-sourcing operations to aid policy suggestions.



Eleftherios Anastasiadis received a BSc in informatics and telecommunications from the University of Athens in 2011. He received an MSC and a PhD in theoretical computer science from the University of Liverpool in 2012 and 2017 respectively.

In 2017 he worked as quality assurance engineer in Rosslyn Data Technologies Ltd. Since 2018 he is a postdoctoral researcher at the Transport Systems and Logistics Laboratory in the department of Civil and Environmental Engineering at Imperial College London. His research interests include approximation algorithms and mechanism design for network optimisation problems, and agent-based simulation for autonomous vehicle fleets.



Marc Stettler is a Senior Lecturer in Transport and the Environment in the Centre for Transport Studies and Director of the Transport & Environment Laboratory. Prior to joining Imperial, Marc was a research associate in the Centre for Sustainable Road Freight and Energy Efficient Cities Initiative at the University of Cambridge, where he also completed his PhD.

His research aims to quantify and reduce environmental impacts from transport using a range of emissions measurement and modelling tools. Examples of recent research projects include: quantifying real-world vehicle emissions; using real-world vehicle emissions data to improve emissions models; evaluating economic and environmental benefits of Kinetic Energy Recovery Systems (KERS) for road freight; and quantifying aircraft emissions at airports. Marc is a member of the LoCITY 'Policy, Procurement, Planning and Practice' working group and the EQUA Air Quality Index Advisory Board.



Panagiotis Angeloudis is a Reader and Director of the Transport Systems and Logistics Laboratory, part of the Centre for Transport Studies and the Department of Civil & Environmental Engineering at Imperial College London. He received an MEng in Civil & Environmental Engineering in 2005 and a PhD in Transport Operations in 2009, both from Imperial College London.

His research interests lie on the field of transport systems and networks operations, with a focus on the efficient and reliable movement of people and goods across land, sea and water. He was recently appointed by the UK Department for Transport to the Expert Panel for Maritime 2050 and was a member of the UK Government Office of Science Future of Mobility review team. He is affiliated with the Centre for Systems Engineering and Innovation, the Institute for Security Science and Technology, the Grantham Institute and the Imperial Robotics Forum.